

**EA Complementary Structural Analysis of Channelized Turbidites in the Offshore Niger Delta:  
Integration of 3D Seismic Data, Inversion of Extra-Deep Azimuthal Resistivity Data,  
Gamma and Density Borehole Images\***

**Chidi N. Ndokwu<sup>1</sup>, Stephen A. Morris<sup>1</sup>, Johanne Paludan<sup>1</sup>, Victor Okowi<sup>1</sup>, Olatunbosun Olagundoye<sup>2</sup>, Nsikak Umoren<sup>2</sup>,  
Arnaud Delpeint<sup>2</sup>, Onyeka Ndefo<sup>2</sup>, Adekunle Agbejule<sup>2</sup>, Richmond U. Ideozu<sup>3</sup>, and Jones E. Acra<sup>3</sup>**

Search and Discovery Article #42352 (2019)\*\*  
Posted February 4, 2019

\*Adapted from extended abstract based on poster presentation given at 2018 International Conference and Exhibition, Cape Town, South Africa, November 4-7, 2018

\*\*Datapages © 2019 Serial rights given by author. For all other rights contact author directly. DOI:10.1306/42352Ndokwu2019

<sup>1</sup>Baker Hughes, a GE Company, United Kingdom ([ndokwuchidi@yahoo.co.uk](mailto:ndokwuchidi@yahoo.co.uk))

<sup>2</sup>Total Upstream Companies Nigeria, Abuja, Nigeria

<sup>3</sup>University of Port Harcourt, Choba, Nigeria

### **Abstract**

Integration of subsurface geological and petrophysical data is necessary for a robust structural interpretation. Complementary structural analysis is a comparative procedure that involves pairing structural interpretations from two or more sources for improved understanding of subsurface structures. The pairing increases the robustness of any structural analysis by providing the geological explanation (type of depositional environment, temporal and spatial considerations), or any other scientific explanation (e.g. tool type, depth of investigation) to support the outcome.

In oil field management, structural analysis of the reservoir provides invaluable information on subsurface structural features (faults, fractures) and reservoir parameters that may impact oil drainage. In this study, a complementary structural analysis scheme was applied to a Middle to Late Miocene channelized reservoir in the Niger Delta area. The reservoir consists of several individual turbidite complexes including stacked channels and extensive, lobate sheet sands. Multiple faults, multi-layered, heterogeneous and discontinuous sand bodies are some of the peculiarities of the reservoir which require characterization for optimum drainage strategy and field management.

This case study shows an integrated structural interpretation from dip measurements derived from inversion of extra-deep azimuthal resistivity data, gamma and density images, and 3D seismic. This has allowed for a better visualization of the near-wellbore structural geology of the wells drilled in the study area, detection of subsurface structural features, discontinuities, and the robust determination of key reservoir parameters (reservoir thickness, geometry) of the drilled channelized sand bodies. Our approach also underscored the importance of complementary structural analysis in the characterization of channelized turbidites during oil field management.

## **Geological Setting of the Study Area**

The study area is located in an oil field in the Niger Delta, in a lease with a sea bed topography that ranges from 1400-1800 m. Several distinct reservoir units deposited during the Middle to Late Miocene occur in the study area. The reservoir consists of several individual turbidite fans including stacked channels and extensive lobate sheet sands. The main reservoir (targeted by Well B in this study) is interpreted mainly as a channelized depositional system consisting of erosive-constructive meandering channels, in an interval of up to 230 m gross thickness with two channel complexes ([Figure 1](#)). The older sequence is called 'Eastern Complex', while the younger is termed 'Western Complex'. Both East and West turbidite complexes have the same characteristic sedimentary evolution, i.e. initial deposition of an erosive-base fairway followed by deposition of erosive-constructive channels. The West Complex overlies the East Complex and develops from it through a major erosive avulsion. Initial deposits are debris flow facies which are made up of impermeable non-reservoir facies that are likely to form a barrier between the East and West complexes. The secondary reservoir (the shallowest reservoir) in the study area is a N-S trending turbidite complex that is interpreted to comprise of an Eastern Channel and a Western Lobe.

Structurally, the oil field structure is a four-way dipping anticline with an axis aligned NE-SW which is located above the lateral ramp of a major thrust, the frontal ramp of which is located approximately 6 km to the southwest of the field where it forms the field's terrace structure. The anticline is divided into a northern and southern part by a reverse fault aligned perpendicular to, and roughly half-way along the axis of the main anticlinal structure. Gentle folding associated with this N-S aligned compression divides the global field's anticline into two smaller four-way dip structures. The structural evolution of the study area is illustrated on the N-S trending seismic line in [Figure 2](#).

## **Description of Data Sources**

This case study focuses on the application of an integrated structural interpretation approach aimed at providing better visualization of the near-wellbore structural geology of the wells drilled in the study area, detection of subsurface structural features, discontinuities, and the robust determination of key reservoir parameters (reservoir thickness, geometry) of drilled channelized sand bodies. Gamma and density images, 3D seismic data, and dip measurements derived from inversion of extra-deep azimuthal resistivity data were employed.

Azimuthal propagation resistivity refers to propagation resistivities that have azimuthal sensitivity and commonly used for geosteering purposes. In this study, the inversion of deep-reading azimuthal propagation resistivity was done with the Multicomponent While Drilling (MCWD) software. MCWD is an algorithm (Sviridov et al., 2014) that can perform real-time processing of any combination of the deep and extra-deep logging-while-drilling (LWD) resistivity measurements, both coaxial and azimuthal. MCWD performs data inversion based on a 1D model. The greatest known challenge of LWD data inversion is the non-uniqueness of the result model. Uncertainty is reduced by constraining the model by taking account a prior knowledge that may come from seismic, adjacent wells and general knowledge about the geological object. The processing is done in short intervals to maintain the fidelity of the subsurface geology. The results from each processing interval include calculated resistivity of the layers detected, distance between the wellbore and the layers, true stratigraphic thickness of each layer, and the relative dip between wellbore trajectory and bed boundaries. The latter is further used to derive apparent dips. The overall visualization is a real-time resistivity model of the drilled interval.

Borehole images can be defined as logs based on the circumferential measurement of a petrophysical parameter along a borehole. Common physical properties used in borehole imaging are gamma, density, resistivity (conductivity), and ultrasonic impedance (Pöppelreiter, García-Carballido, and Kraaijveld, 2010). Borehole images used for this study were acquired on a logging-while-drilling (LWD) platform using bulk-density imager and gamma-ray imager tools. From the borehole images acquired in the high-angled wells, structural features were identified, categorized and measured from planar surfaces that intersect the borehole. A sine wave was manually fitted to these features (manual-dip picking) since manual-dip picking allows the interpreter to distinguish between feature and artefact, and also allows each feature to be classified into a specific geological category (e.g. bedding plane or fault). Specific steps in a workflow were followed (QC of raw field data, manual-dip picking, feature identification, orientation, domain definition, dip anomaly identification, etc.) aimed at obtaining a valid structural interpretation.

Seismic sections are 2D images of the subsurface that are extracted from a 3D seismic data volume. Depending on the interpretation context, seismic sections can be used for structural, stratigraphic, and/or fluid interpretation (Bacon, Simm, and Redshaw, 2003). According to Dorn (1998), 3D seismic data provide constraints for detailed reservoir characterization, planning and executing enhanced oil recovery strategies, and reservoir monitoring. For example, stratigraphic and subsurface structural features (faults or fractures) that may impact oil drainage can be discerned from seismic data. 3D seismic data is also the primary input that is used to aid reactivity when drilling in turbidite environments, where the lateral discontinuity of sand bodies arising from faulting and peculiarities of the depositional environment pose challenges during the placement/geo-steering of high angle and horizontal wells. During drilling, seismic data is often paired with data from other sources (e.g. borehole images, petrophysical logs, extra-deep-reading azimuthal resistivity data) to guide the structural analysis of subsurface features. A robust structural analysis is invaluable in the design and implementation of an optimum drainage strategy in field development.

## **Applications of the Integrated Structural Interpretation Approach**

### **Well 1**

#### Near-Wellbore Features

The relative dips from LWD borehole image were compared with that from MCWD inversions ([Figure 3](#)). The former has bulk density as the main measuring parameter, while the latter processed extra deep-reading azimuthal propagation resistivity readings. The comparison showed similar trend and values except a few high-angled features (faults and lithological boundaries) interpreted from the borehole image. The high-angled features were not captured by MCWD inversion relative dips because the process is 1-D. MCWD captured these high-angled features mostly in the form of higher misfits for the intervals. Misfit is a measure of inversion being successful; a good match between synthetic and actual curves gives the lowest misfit.

#### Structural Discontinuities

A cumulative dip plot ([Figure 4](#)) was used as a tool to support the interpretation from borehole image. From seismic interpretation, a major fault was expected at 4343 m MD (2474 m TVDSS), but encountered at about 4330 m MD (2471 m TVDSS). The drag zone for this major fault is a short interval and no clear fault plane was observed ([Figure 5](#)).

### Elements of Reservoir Architecture

Well 1 was drilled as a producer into a turbidite complex made up of a channel and lobe. [Figure 6](#) shows the seismic representation of the geologic structure (faults, sand body geometry, thicknesses, bed boundaries, etc.) along the well bore. On seismic, two structural panels (1 and 2) are clearly evident based on the significant throw exhibited by the fault F1. In the field, this fault has a major impact on reservoir connectivity due to its significant throw. Lithological and depth prognosis was driven by seismic reservoir characterization interpretation and reference wells.

In addition, 3D seismic data was the primary data used in deducing the geologic/subsurface model that served as the initial input for geosteering model. Information from the seismic interpretation was complimented by borehole imaging and MCWD inversion ([Figure 7](#)) during well geosteering to optimize sand length in each panel (net sand of 430 m MD vs. Base Case 580 m MD). The realized sand length was considered optimal since it is sufficient to achieve Well A's objective of 15 kbpod. Moreover, in areas where the reservoir was shallower than expected, complimentary structural analysis from borehole imaging and the integrated interpretation of the multiple sources of data ensured better understanding of the subsurface geology.

## **Well 2**

### Near-wellbore Features

Well 2 is a case of highly faulted and discontinuous sand bodies. Comparing the relative dips from MCWD inversion and borehole image interpretation ([Figure 8](#)) showed similar trend and values at some shaly zones (about 3860-4075 m MD; 4088-4120 m MD; 4392-4448 m MD; 4595-4655 m MD), and dissimilar trend at some sand bodies and other high-angled features (faults and lithological boundaries). The mismatches can be correlated to intervals of high misfit in MCWD inversion or paucity of dip picks in sand bodies. The obvious mismatch seen from 4800m falls into the interval of zone 2 in structural zonation ([Table 1](#)). This zone is characterized by thin beds ([Figure 9](#)) and MCWD's model approximation leads to higher misfits.

### Structural Discontinuities

A structural interpretation was completed between 3645 m and 5340 m measured depth (MD) (see summary in [Table 1](#)). The structural features identified include bedding planes, lithological boundaries and faults. Two structural zones were identified based on the preferred bedding orientation of the formation drilled through. Zone 1 is from 3645 m to 4803 m MD and the average dip orientation read 7/209. Zone 2 is from 4803 m to 5340 m MD and the average dip orientation read 15/295. The high-angled features coincided with and gave confidence to geosteering interpretation of fault position. These high-angled features trend in the same manner as that recorded in field studies that are characterized by dominant NE-SW normal faults developed as a consequence of the onset of a deep duplex.

### Elements of Reservoir Architecture

Well 2 was drilled to produce oil from a turbidite complex. The main target reservoir is a channel found in the Lower Complex, while secondary targets were two channels. [Figure 10](#) highlights the subsurface structure and stratigraphy (i.e. faults, sand body geometry, thicknesses, bed boundaries, contacts, etc.) as deduced from 3D seismic interpretation. On seismic, six structural panels (1 to 6) have been interpreted based on the significant throws exhibited by faults along the well trajectory. These faults have major impacts on reservoir

connectivity due to their significant throws; hence it was crucial that sufficient sand lengths were encountered by Well B in each panel. During well planning, lithology and depth prognosis was done using seismic reservoir characterization and reference wells.

As implemented in the Well 1 Case Study, 3D seismic data served as the main data in deducing the geologic/subsurface model that was used as the initial geosteering model. The seismic interpretation was also complimented by borehole imaging and MCWD inversion during well geosteering to optimize sand length in all the panels ([Figure 11](#)). A net sand of 1190 m MD vs. base case 400 m MD was realized, with sufficient sand encountered in each panel to ensure pressure support from the associated water injector.

### **Conclusions**

This case study focused on the pairing of structural interpretation from different sources – 3D seismic, borehole image and azimuthal resistivity. This integration enriched the understanding of the reservoir in terms of structural zones, discontinuities, and geometry. Qualitatively, the different interpretations showed similar trends. Major structural discontinuities and inversion interval length were the causes of variation in interpretations. The integration of structural interpretation from dip measurements derived from inversion of extra-deep azimuthal resistivity data, azimuthal gamma and density logs, and 3D seismic interpretations allowed for better visualization of the near-wellbore structural geology, detection of subsurface structural features, and the determination of key reservoir parameters (reservoir thickness, geometry) of the drilled channelized sand bodies. Our approach underscored the importance of complementary structural analysis in the characterization of channelized turbidites during oil field management. Further studies should focus on a quantitative comparison to estimate the degree of variance in values and its relation to geology, procedure, and software.

### **Acknowledgements**

The authors thank Total Upstream Companies Nigeria, Lease Partners, and Baker Hughes (a GE company) for the permission to publish this article.

### **Selected References**

Bacon, M., R. Simm, and T. Redshaw, 2003, 3-D Seismic Interpretation: Cambridge University Press, 212 p.

Dorn, G.A., 1998, Modern 3-D seismic interpretation: The Leading Edge, v. 17/9, p. 1262-1272.

Pöppelreiter, M., C. Garcí'a-Carballido, and M. Kraaijveld, eds., 2010, Dipmeter and borehole image log technology: AAPG Memoir 92, 357 p.

Sviridov, M., A. Mosin, Yu. Antonov, M. Nikitenko, S. Martakov, and M.B. Rabinovich, 2014, New Software for Processing of LWD Extra Deep Resistivity and Azimuthal Resistivity Data: SPE-160257-PA.

Yared, K., M. Pelorosso, D. Buster, I. Altintutar, E. Manuel, J. Doyle, and C. Russell, 2010, Novel Approach to Quantifying Deepwater Laminated Sequences Using Integrated Evaluation of LWD Real-Time Shear, Porosity, Azimuthal Density and High-Resolution Propagation Resistivity: SPE 134515.



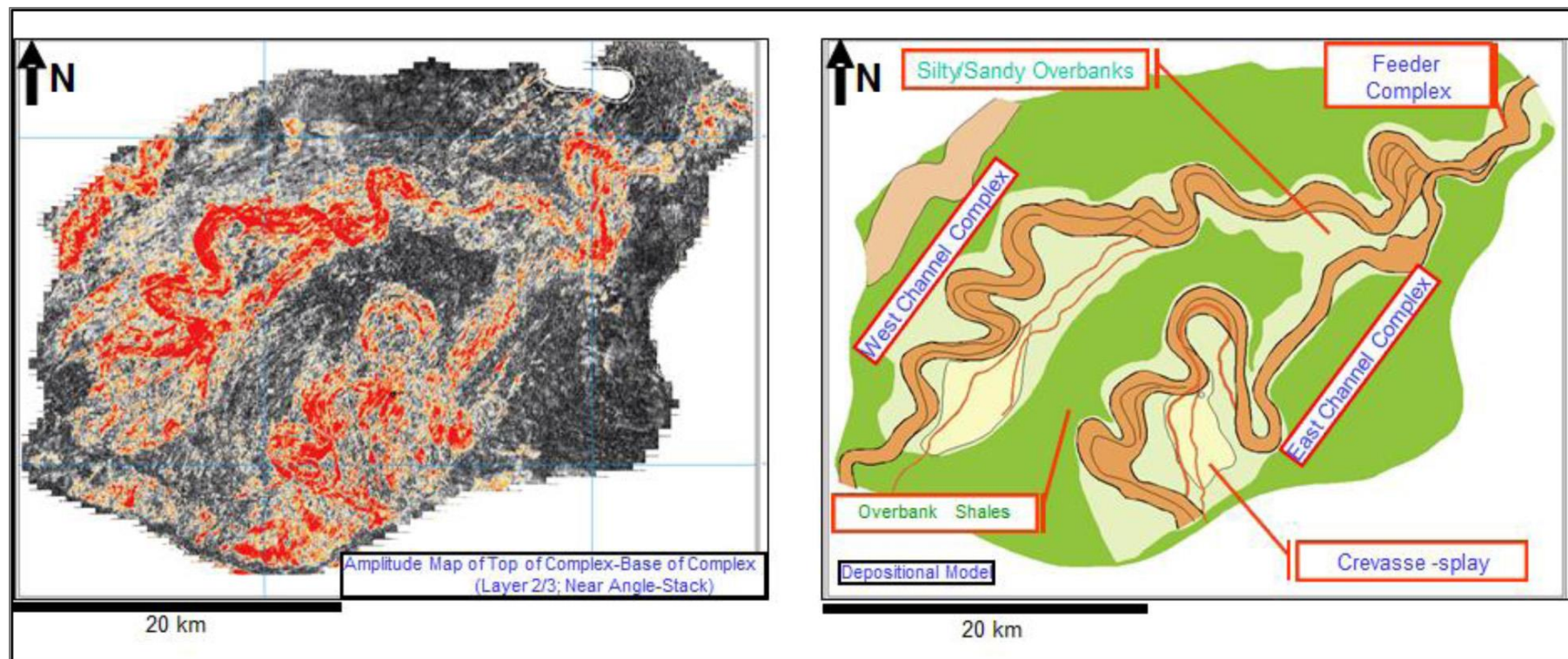


Figure 1. Amplitude map and corresponding depositional model of the East and West Channel complexes of the main reservoir in the study area.

## 2 main structural phases:

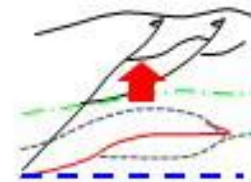
### 1 H1120-H930 (Tortonian)

Shallow detachment activation → Shallow thrust system onset

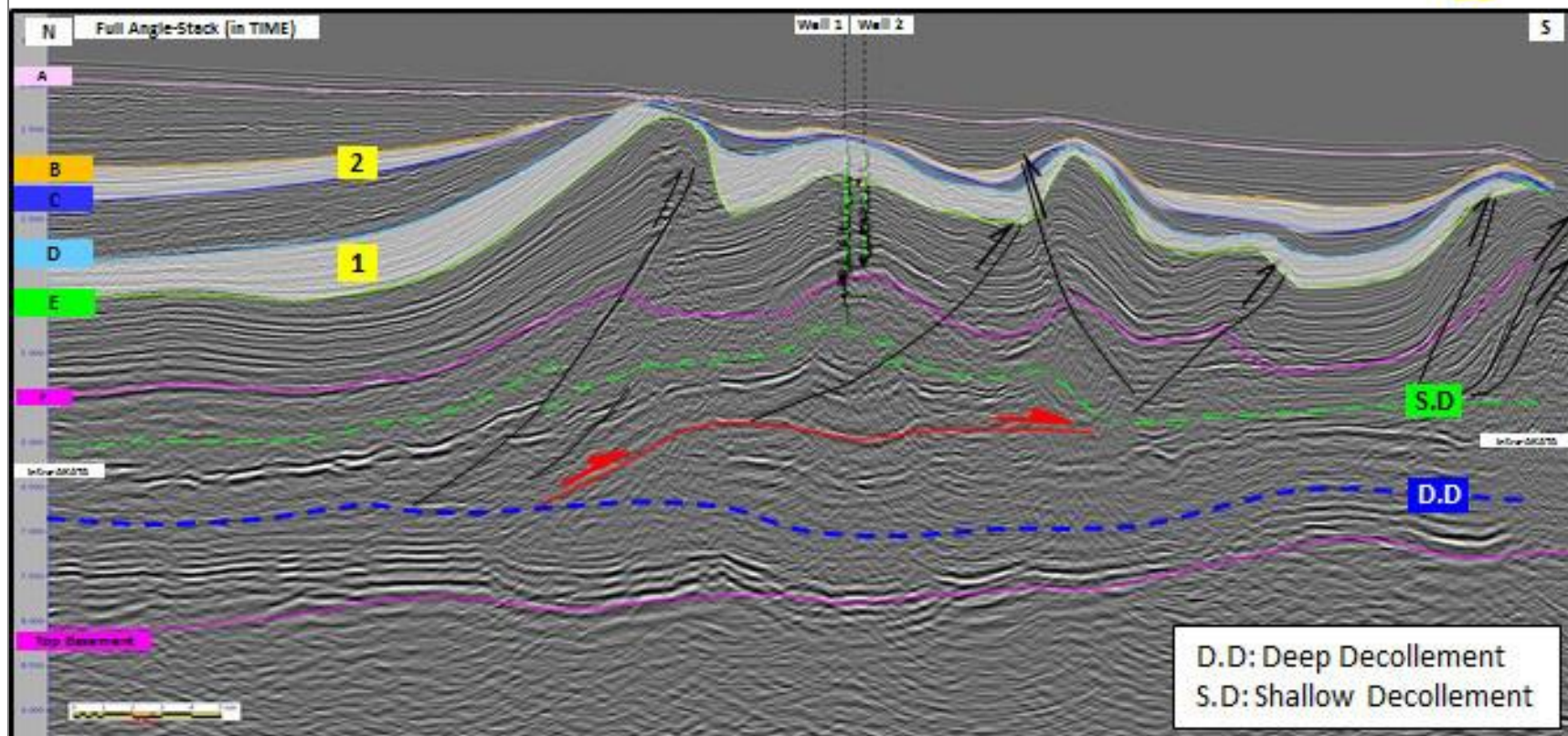
### 2 H930-H400 (Messinian – Pliocene)

Deep detachment activation → Deep thrust sheet emplacement

1<sup>st</sup> occurrence of deep structures ~9Ma (D Horizon)



1



2

Figure 2. North-South seismic line showing the structural evolution of the study area.



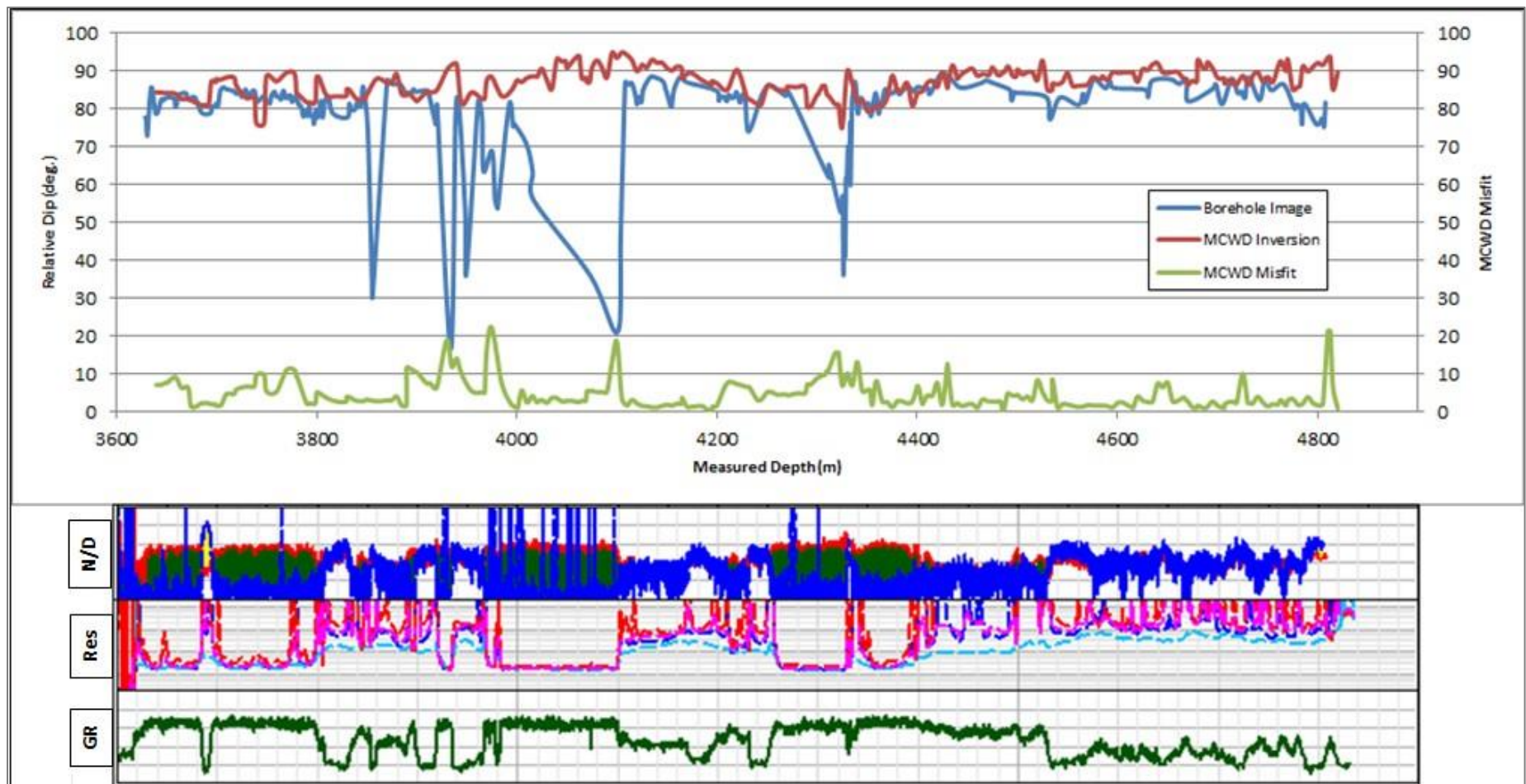


Figure 3. A comparison plot between relative dips from LWD borehole image and MCWD inversion. Relative dip refers to the angle between a line normal to the bedding plane and the wellbore axis measured in their common plane.



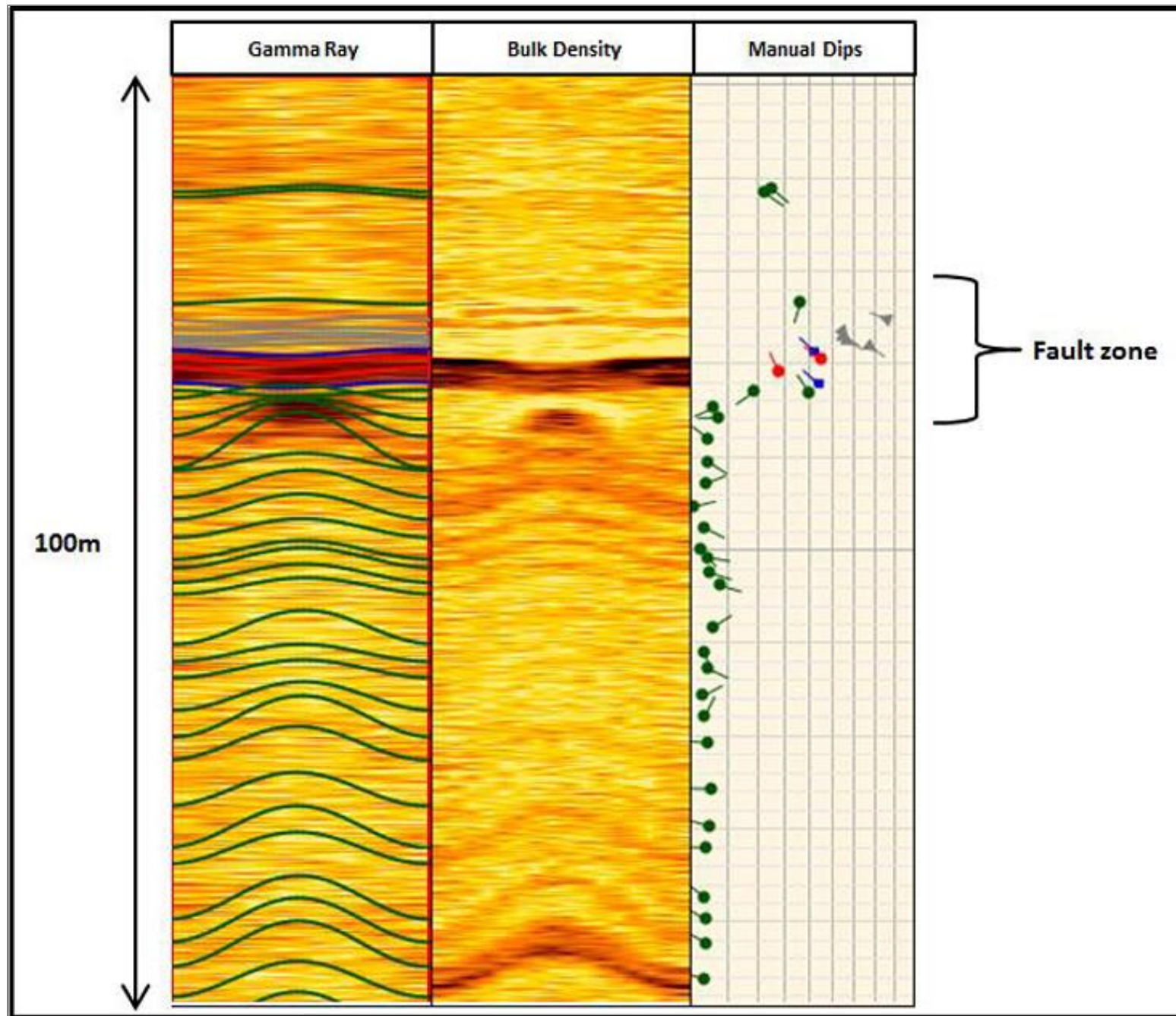


Figure 5. High-angle features in the fault zone and adjacent drag zone.



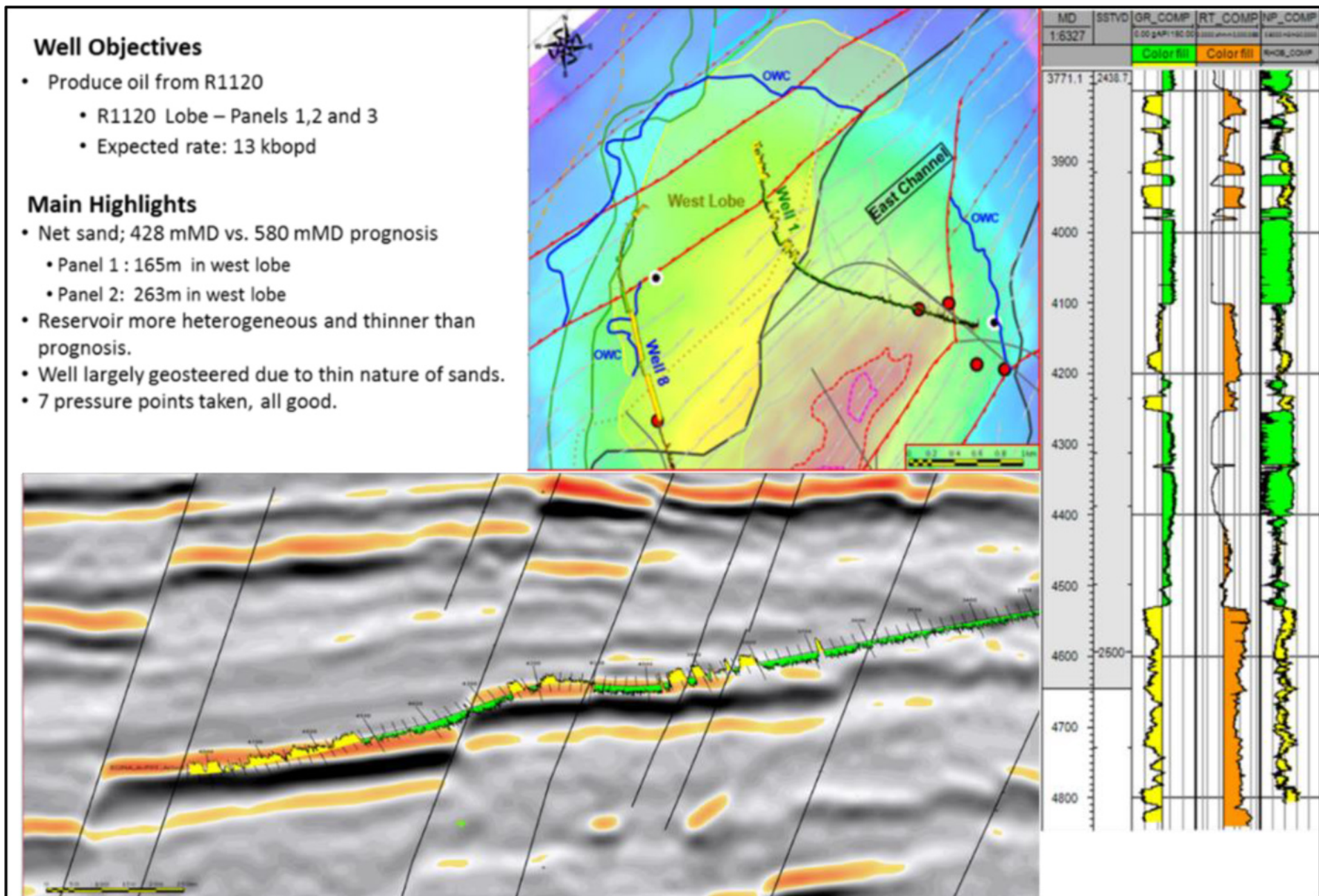


Figure 6. Seismic section along realized trajectory.



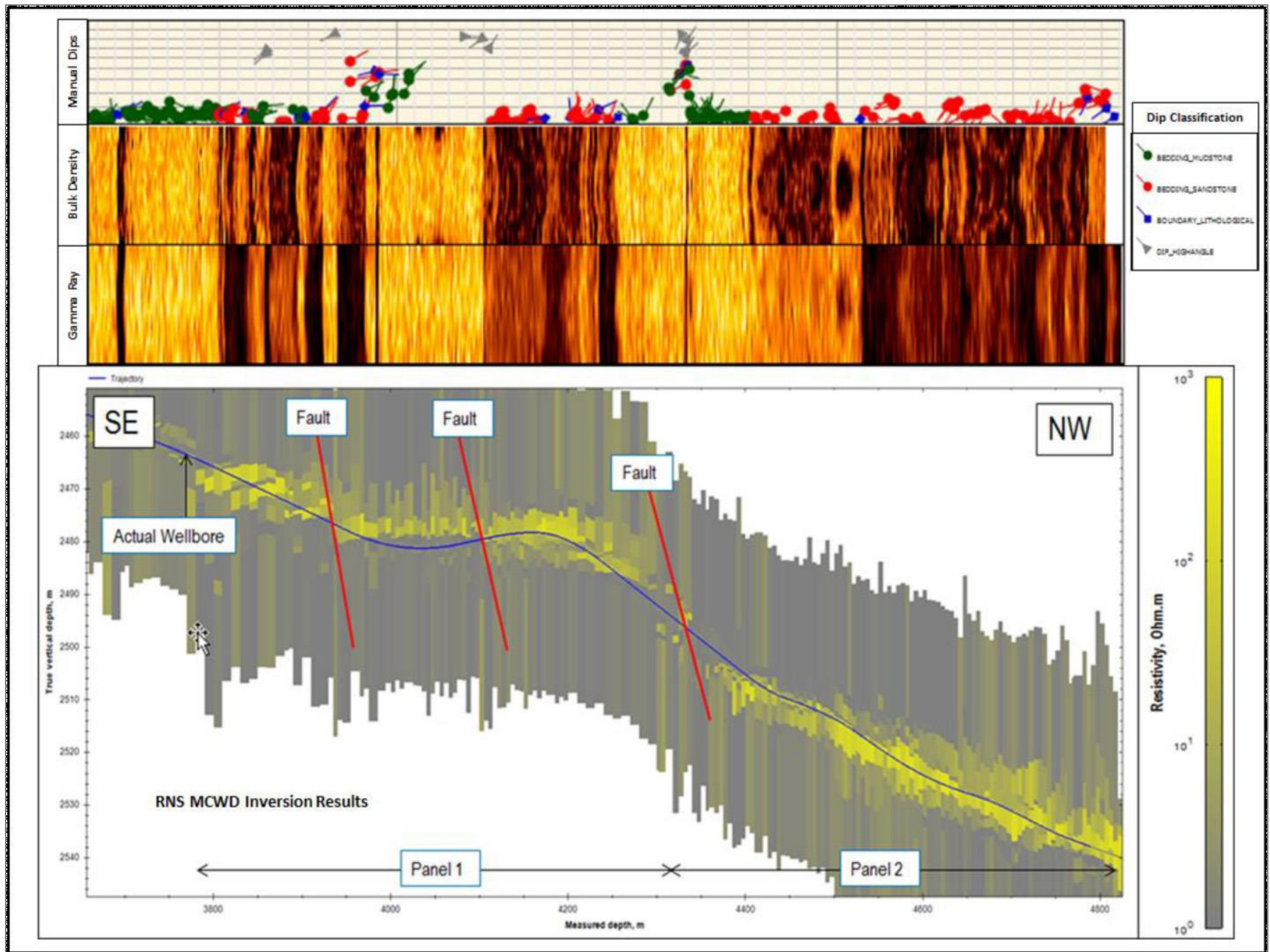


Figure 7. Borehole image juxtaposed with MCWD inversion results.

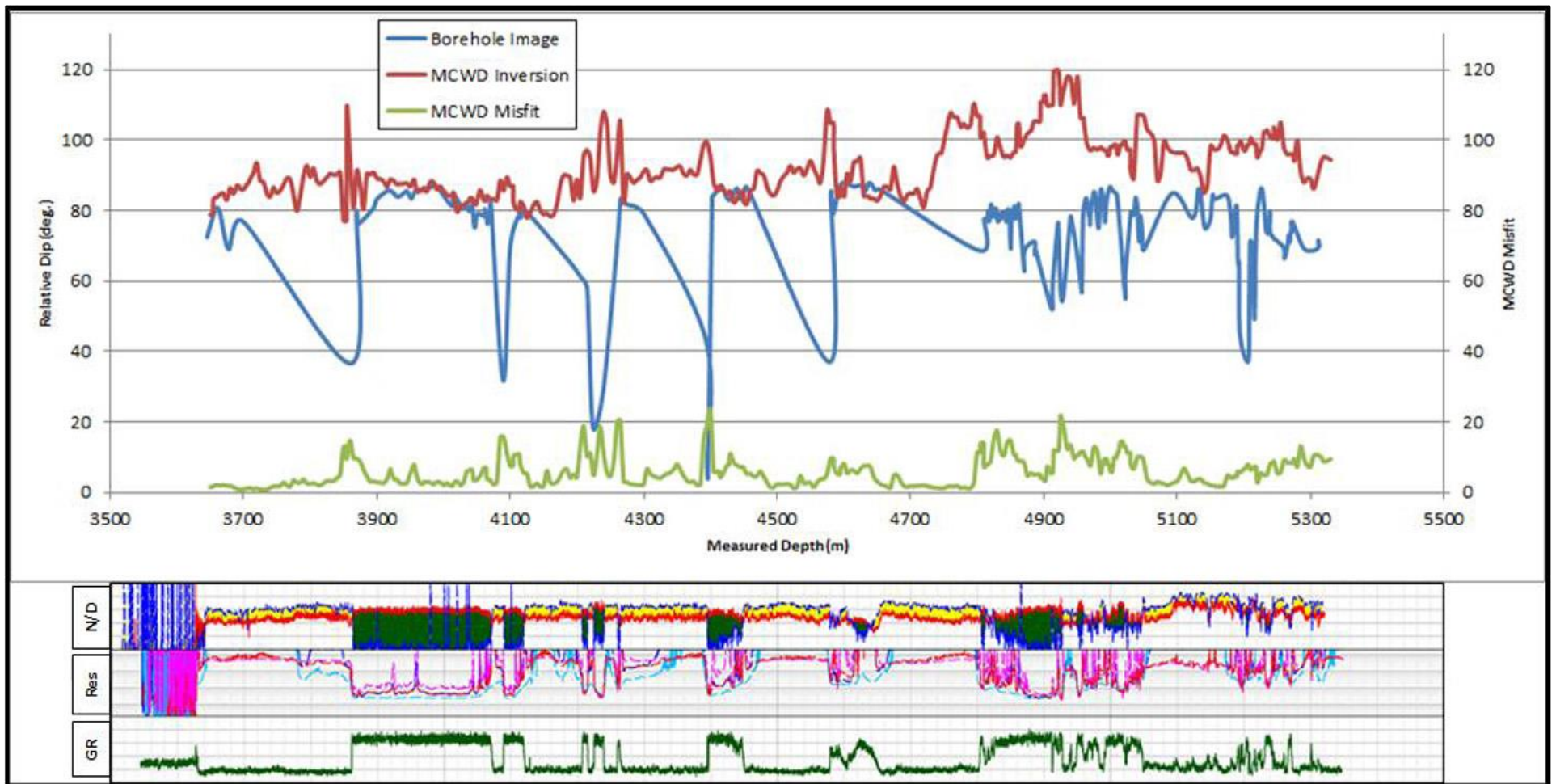


Figure 8. A comparison plot between relative dips from LWD borehole image and MCWD inversion.

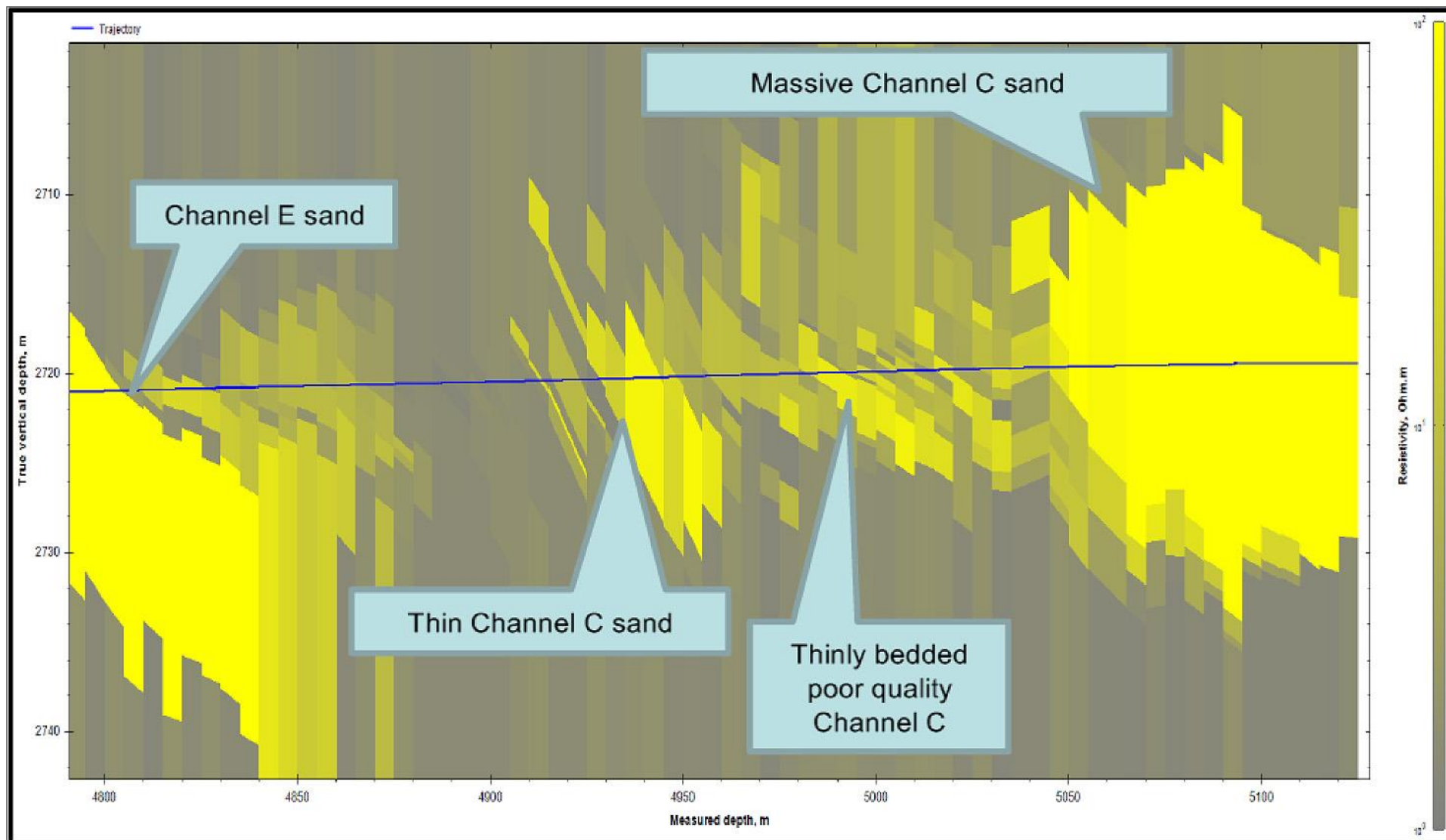


Figure 9. MCWD resistivity model showing thinly bedded and discontinuous sand bodies.



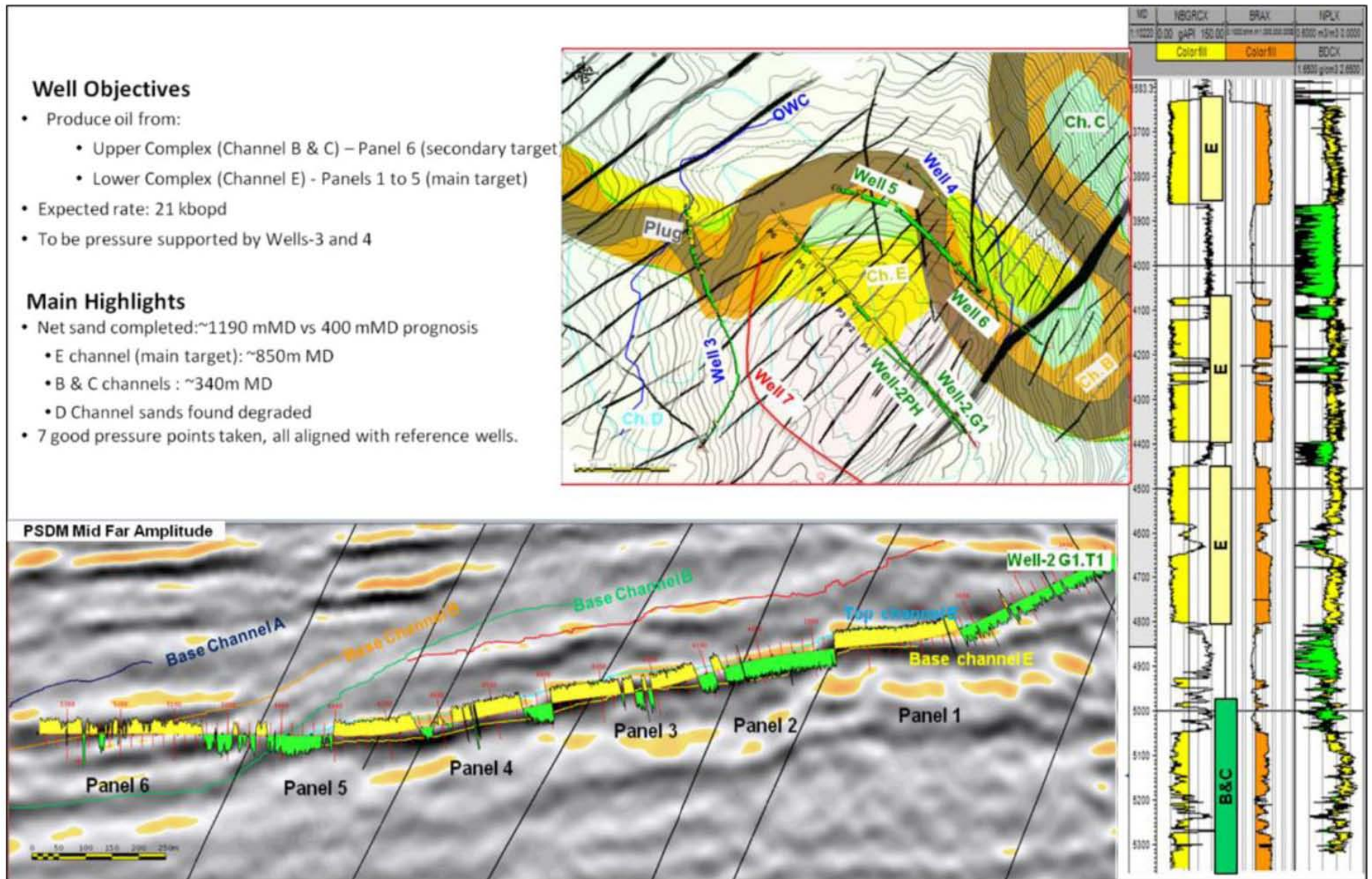


Figure 10. Seismic section along realized trajectory juxtaposed with well results.



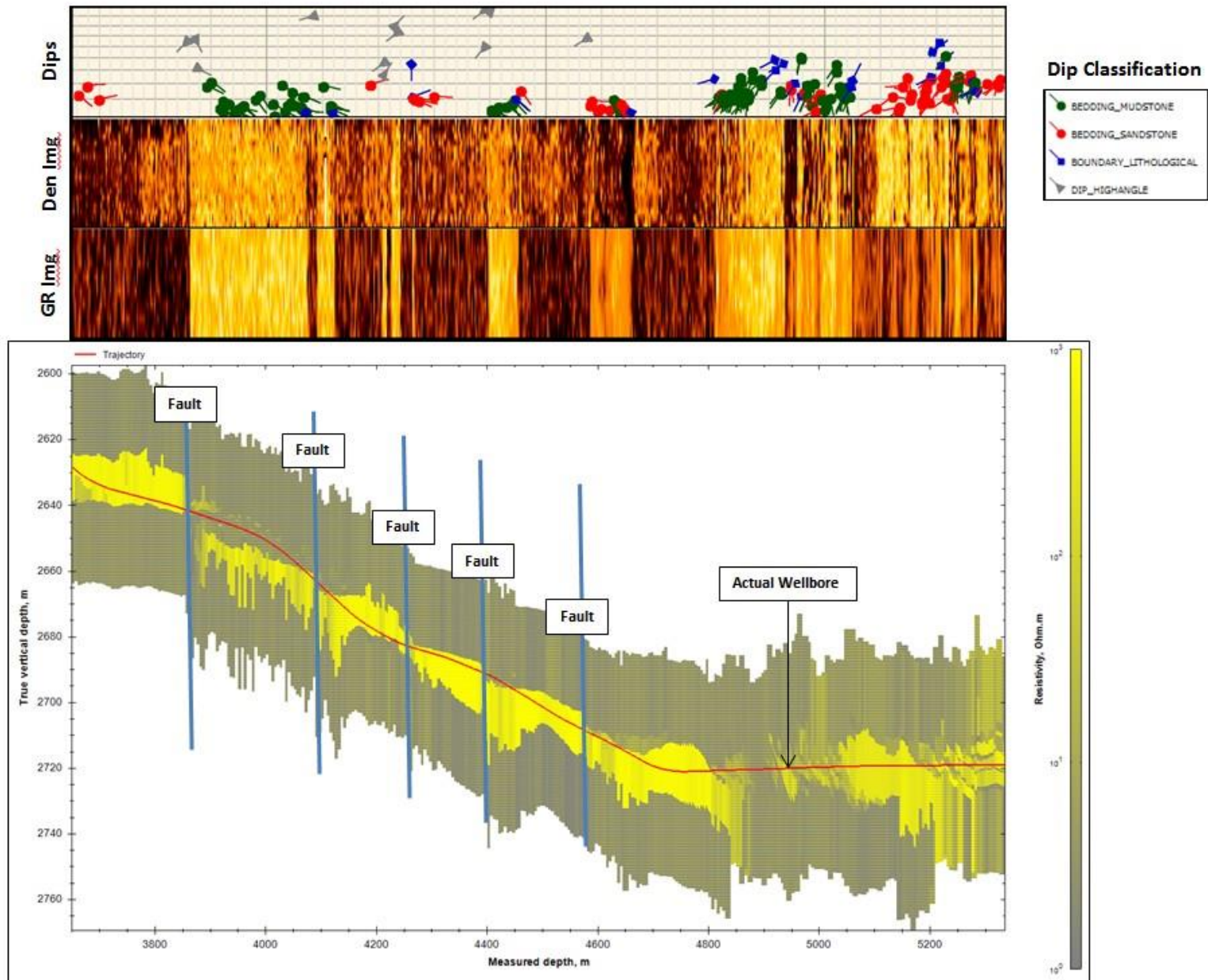


Figure 11. Borehole image juxtaposed with MCWD inversion results.

Structural Zone	Measured Depth (m)	Mean Structural Dip (deg.)	Comments
1	3645 - 4803	7/209 (n=64)	Low dip values for mudstone and sandstone in Channel E sand; SSW preferred dip direction; multiple high-angled features.
2	4803 - 5340	15/295 (n=114)	Relatively more bed boundaries; from intercalated interval to a massive Channel C sand and then Channel B sand; WNW preferred dip direction.

Table 1: Summary of structural interpretations.